HETEROCYCLES, Vol. 102, No. 6, 2021, pp.1061-1082. @ 2021 The Japan Institute of Heterocyclic Chemistry
Received, 22nd August, 2020, Accepted, 2nd November, 2020, Published online, 9th November, 2020
DOI: 10.3987/REV-20-943

SYSTEMATIC SEARCH FOR TRANSITION STATES IN COMPLEX MOLECULES: COMPUTATIONAL ANALYSES OF REGIO- AND STEREOSELECTIVE INTERFLAVAN BOND FORMATION IN FLAVAN-3-OLS

Daisuke Urabe* and Keisuke Fukaya

Biotechnology Research Center and Department of Biotechnology, Toyama Prefectural University, 5180 Kurokawa, Imizu, Toyama 939-0398, Japan. E-mail: urabe@pu-toyama.ac.jp

Abstract – This review describes our recent work on a systematic search for transition states in transformations of complex molecules. The method features a combination of a conformational search method using constrained models to create a large library of transition-state candidates, and subsequent density functional theory (DTF)-based transition state calculations for the candidates. The method is applicable to calculation of transition states for inter- and intramolecular interflavan bond formation in flavan-3-ols to reproduce experimental results for highly regio- and stereoselective C-C bond formation. The specific roles of van der Waals interactions in the transition states can be visualized by NCIPLOT mapping to show the importance of weak but attractive interactions for selective interflavan bond formation.

CONTENTS

1. INTRODUCTION

Quantum chemical calculations are widely used in the field of synthetic organic chemistry, where chemists attempt to discover unique and unexpected structures, determine the reactivity of organic molecules, and predict their applications to natural product synthesis, reaction development, and design and synthesis of organic materials and supramolecules. Computing molecular properties such as preferable geometries, energies, molecular orbitals, and electronic properties provides valuable information to chemists for implementation in theoretical research. The synergetic interplay of synthetic chemistry and computational chemistry is essential for exploring the cutting edge of organic chemistry.

Calculation of transition states provides novel insights related to molecular reactivity based on thermodynamic parameters, and thus enables a deeper understanding of reaction pathways.[1,2] In the field of natural product synthesis, transformation mechanisms including chemo-, regio-, and stereoselective reactions are investigated by computational analysis of transition states to rationalize the formation of products[3] and to design intermediates for key transformations to the target products.[4,5] The use of computational chemistry in mechanistic studies of transformations[6] mediated by transition metals,[7] organocatalysts,[8] and enzymes[9] is now accepted as a standard approach for the development of new reactions, and further applications to the rational and automatic design of ligands and catalysts has been widely explored.[10]

The application of transition state calculations to the analysis of transformations of highly functionalized molecules is still challenging, despite many successful examples to date, because the search for transition states becomes more difficult as the structure of target molecules becomes complex. Although synthetic chemists are interested in calculating transition states of complex molecules, it may be difficult to perform such calculations without sufficient training. Usually, reaction mechanisms are considered using a simplistic approach involving handwritten structures, so that the intricate behavior of complex molecules is not resolved.

We have previously reported computer-aided mechanistic studies on unique transformations encountered in the total synthesis of natural products.[11] Visualization of the three-dimensional (3D) structures of transition states, and evaluation of favorable pathways by comparison of the energies of competing transition states that lead to different products, has enabled an objective discussion of reaction

mechanisms, and has sometimes revealed the hidden reactivity of synthetic intermediates. On the other hand, calculation of transition states for the reactions of complex molecules, particularly flexible molecules, has not been an easy task, because of the presence of conformational isomers in the transition states. This situation has led us to consider the importance of a simple and systematic transition state search applicable to complex molecules.

Recently, we reported an effective method to search for transition states by targeting regio- and stereoselective interflavan bond formation in flavan-3-ols during the total synthesis of naturally occurring complex flavonoids, the procyanidin B series.[12] This method could provide transition states from a considerable amount of conformationally isomeric transition states that could reproduce the experimental results for inter- and intramolecular interflavan bond formation. In this review, we summarize the transition state search method, and describe mechanistic studies on three types of regio- and stereoselective interflavan bond formation.

2. CONFORMATIONAL EFFECTS ON ENERGY OF TRANSITION STATES

The first task is the creation of an appropriate initial geometry in an input file to, in order to calculate transition states. The goal of the calculation is to find a saddle point starting with an initial geometry. The use of an unsuitable initial geometry will cause the calculation to fail. Therefore, creation of an accurate initial geometry is important for the success of the transition-state calculation. Although highly efficient methods such as anharmonic downward distortion following (ADDF), artificial force-induced reaction (AFIR),[13] nudged elastic band (NEB),[14] and ab-initio molecular dynamics (AIMD)[15] have been employed to find saddle points and the minimum energy path, it is still necessary to perform trial-and-error calculations for large complex molecules.

When a transition state is determined after trial-and-error calculations, it can still be unclear whether the obtained geometry is the lowest-energy transition state among all conformational isomers. Even if the mechanism involved in the target reaction is clear and simple, the possibility of the presence of a more conformationally stable isomeric transition state on the potential energy surface cannot always be ruled out. Unless the transition state with the lowest-energy conformation is obtained, it is unclear whether the energy difference between competing transition states that lead to different products is associated with the difference between the desired and undesired pathways, or with conformational factors.

Figure 1 shows an example of the conformational effect on transition states for the intramolecular Diels-Alder reaction of **1**, which provides the 8/6-bicyclic compound **2**.[16] Based on the preferred conformations of cyclooctane, two possible transition states can be identified for the cycloaddition when R = H (**1a**). These adopt the boat-chair and chair-chair forms **TS-A** and **TS-B**, respectively, for the formation of an 8-membered ring, and the calculated energy of the two transition states is almost the same

($\Delta\Delta G$ = 0.02 kcal/mol). In contrast, if a methyl group is used instead of a H group (R = Me, **1b**), a marked difference in the stability of the boat-chair and chair-chair transition states **TS-C** and **TS-D** is observed, and the chair-chair transition state **TS-D** is predominant ($\Delta\Delta G$ = 7.0 kcal/mol). Therefore, to consider the energy barrier for the cycloaddition of **1b**, we have to model the chair-chair transition state, because the use of the boat-chair transition state would lead to an incorrect result.

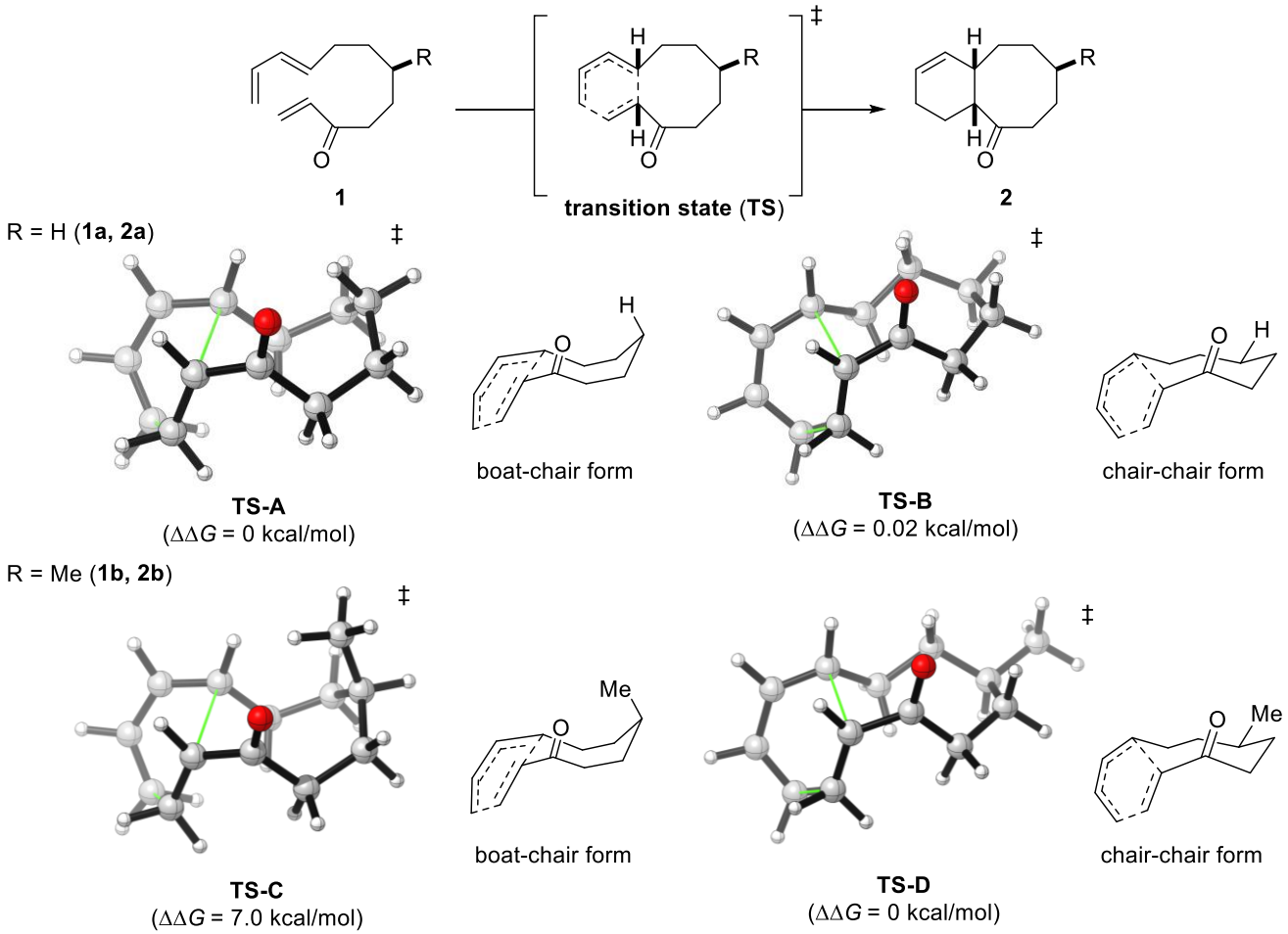

Figure 1. Conformational effect on energy of transition states for Diels-Alder reaction of **1**

In this simple case, we can easily predict the large energy gap between the boat-chair and chair-chair transition states **TS-C** and **TS-D** without any calculations, because there is a clear steric repulsion between axial Me and H groups in the boat-chair form of the 8-membered ring. Therefore, when making an input file, modeling of the boat-chair-like geometry as the initial structure can be avoided for the transition-state calculation, and only the chair-chair-like geometry is modeled to obtain the minimum-energy transition state. On the other hand, when substrates become more complex due to the presence of other substituents, the preferred conformation of the formed ring, i.e., the preferred conformation of the transition state, is unclear. Therefore, a suitable input geometry cannot be found.

In this situation, the transition-state calculations should be coupled with a conformational search for transformations of the complex molecules. An effective means of achieving this is the use of a Monte Carlo method to create a library of initial geometries. A search of the resulting model compounds, based on suitable bond lengths, can generate many conformational isomers that have an appropriate geometry for transition-state calculations, which cannot be determined from the 2D structures of either the reactant or the product. This can provide multiple possible isomeric transition states, and the energetically favorable candidate can then be identified.

3. TRANSITION STATES FOR DIMERIZATION OF FLAVAN-3-OLS

3-1. Studies on Synthesis of Procyanidins by the Saito and Nakajima Group

Flavonoids are a class of plant-derived secondary metabolites, and are common in foods such as fruits, vegetables, and teas.[17] This family exhibits a broad range of bioactivity, including anti-oxidant, anti-inflammatory, and anti-tumor activity; therefore, the dietary intake of food rich in flavonoids is considered to be beneficial to human health.[18] Catechin and epicatechin (a C3-epimer of catechin, Figure 2) are poly-oxygenated flavan-3-ols that serve as monomers of oligomeric flavonoids, referred to as procyanidins.[19] Among the procyanidin family, the procyanidin B series is characterized by a dimeric structure of flavan-3-ols, which are connected by C4-C8′ or C4-C6′ interflavan bonds. The C3-epimeric configurations in the flavan-3-ols and the two types of interflavan bonds diversify the structures of the procyanidin B series to eight isomeric compounds, procyanidins B1-B8, all of which are found in nature (Figure 2). Although the slight structural differences in the procyanidin B series complicate purification from natural sources, stereoselective total synthesis enables the production of pure procyanidins B1-B4, for which anti-oxidant activity has been demonstrated.[20]

The complex structures of the procyanidin B series have inspired synthetic chemists to develop methods for constructing the dimeric structure of flavan-3-ols.[21] Over the past decades, the Saito and Nakajima group has reported a versatile approach to the coupling of flavan-3-ols under Lewis acidic conditions.[22-24] Scheme 1 illustrates a general view of their synthetic approach. Protected flavan-3-ol **3** is designed as an electrophilic fragment by placing the ethoxyethyl acetal (OEE) leaving group at the C4 position. Thus, Lewis-acid treatment of **3** effectively generates carbocation intermediate **4**. A subsequent Friedel-Crafts-type reaction of the A′-aromatic ring in flavan-3-ol **5** as a nucleophilic fragment forms the interflavan bond. This is followed by deprotonative rearomatization from Wheland intermediate **6**/**8** to deliver the dimeric flavan-3-ols **7**/**9** as advanced intermediates to produce the procyanidin B series.

To synthesize each isomer of the procyanidin B series by this method, the formation of interflavan bonds should be implemented in a regio- and stereoselective manner. For the synthesis of procyanidins B1-B4, regioselective formation of C4-C8′ bonds is required, while C4-C6′ bonds must be formed for

procyanidins B5-B8. With respect to the C4-stereoselectivity, the newly formed interflavan bonds should be *trans* to the adjacent C3-hydroxy groups in all cases. Assuming that the final rearomatization is a rapid and irreversible process, C-C bond formation would be the most crucial regio- and stereo-determining step for the selective synthesis of the procyanidins.

The Saito and Nakajima group succeeded in completely controlling the regio- and stereoselectivities of interflavan formation by taking advantage of the poly-oxygenated structures of flavan-3-ols. They employed several protecting groups including Bn, TBS, and acyl groups not only to mask the hydroxy groups, but also to alter the reactivity of the monomers to obtain the desired coupling in an inter- and intramolecular manner, and to achieve the total syntheses of procyanidins B1-B4 and B6, and C4-epi-procyanidin B3.

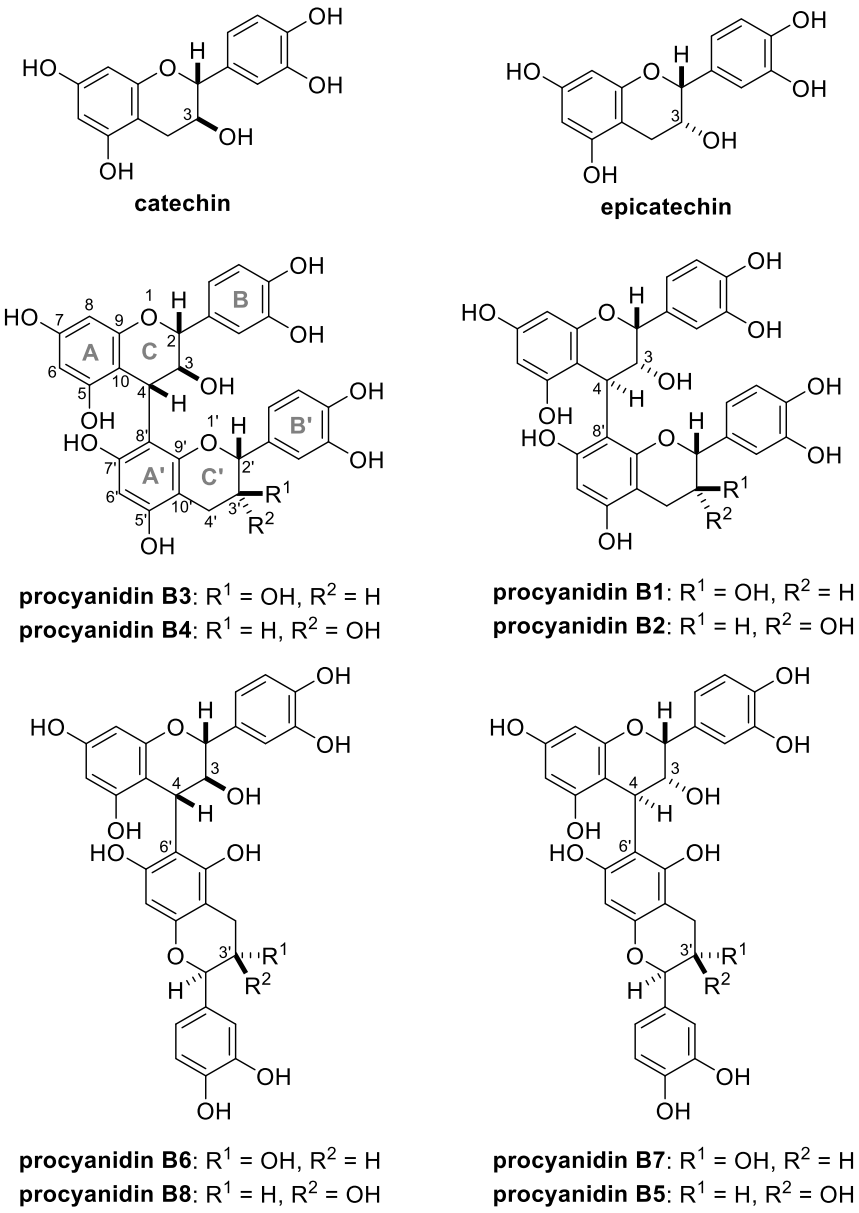

Figure 2. Structures of catechin, epicatechin, and procyanidin B series

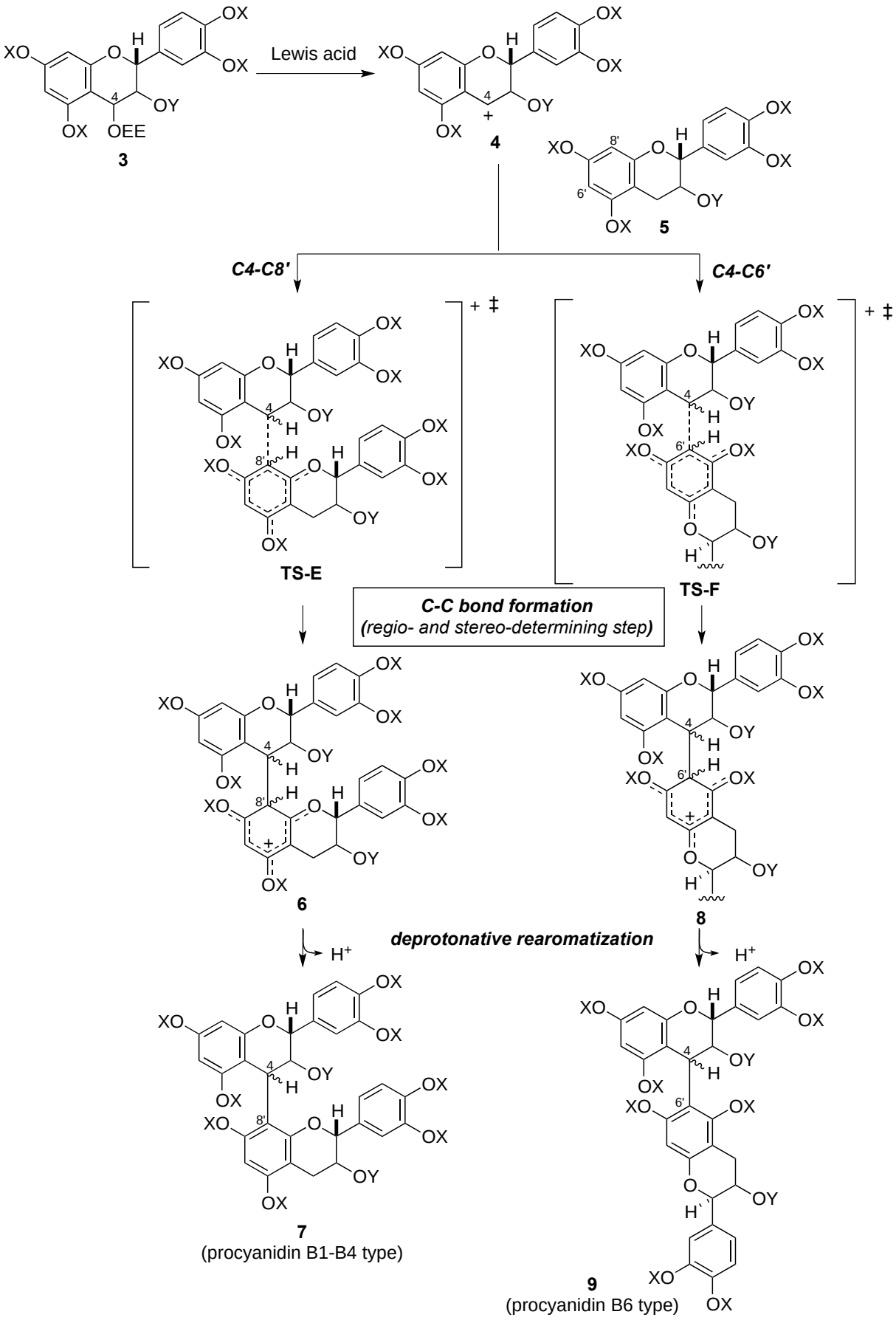

Scheme 1. General mechanism for Lewis acid promoted coupling of flavan-3-ols

3-2. Protocol for a Systematic Searching for Transition States

Regio- and stereoselective interflavan bond formation in flavan-3-ols is expected to be controlled by the steric and electronic biases from the C3 and C3′-stereocenters and multiple functional groups. As for the C4-stereoselectivity, the C3-substituent of electrophile **4** may enforce the nucleophilic approach of **5** from the opposite face to lead to a *trans* relationship between the C3 and C4-substituents. However, the regioselectivity is not easily rationalized because both the C8′ and C6′ carbons are equally activated by the two *ortho* and one *para* oxygen functionalities, and thus the two positions appear to have similar nucleophilic properties. The steric environment at C6′ and C8′ also appears similar enough to be indistinguishable.

The difficulty in the identification of the specific reason for the high selectivities from the 2D structures of the complex flavan-3-ol derivatives has provided insight into the importance of the conformational preference of the transition state **TS-E**/**TS-F**, whose energy would affect the selectivities for C-C bond formation. This hypothesis led us to perform a computational analysis of the experimentally determined interflavan bond formation results reported by the Saito and Nakajima group, and to develop a method for systematically searching for transition states.

A conformational search using molecular mechanics and geometry optimization with semi-empirical molecular orbital (MO) and density functional theory (DFT) methods was exploited to systematically generate conformational isomers for the transition states.[25] The process flow for the transition-state search used for the analysis of the regio- and stereoselectivities involved in the coupling of flavan-3-ol derivatives is shown in Scheme 2. The first step is to model the target transition states in an appropriate form for the calculations (Step 1). Some substituents (Bn or TBS groups) that are not expected to participate in the reaction are replaced with simpler substituents (H or TMS groups). Although this should be avoided if possible, it leads to a reduction in the computation cost by simplification of the structure of large molecules. The lengths of the C4-C8′ and C4-C6′ bonds are thus constrained to 2.1 Å. The model is subjected to a Monte Carlo conformational search using molecular mechanics (OPLS3e) to generate a large amount of conformational isomers for the constrained model (Step 2). The conformers with energies within 5 kcal/mol from the minimum value are then selected for the next step of the calculation. The geometries of the conformers are refined by semi-empirical MO calculations (PM6) while keeping the length of the forming bond at 2.1 Å, and identical structures are then removed based on the root-mean-square deviation (RMSD) values (Step 3). The obtained geometries are subjected to transition-state calculations by the DFT method (e. g. B3LYP-D3BJ/6-311+G(d,p)-PCM//B3LYP-D3BJ/6-31G(d)-PCM) to generate a library of plausible transition states for C-C bond formation (Step 4). From the superposed structure of the obtained transition states, this procedure is

confirmed to comprehensively cover conformational isomers. The optimized transition states are classified into clusters that lead to possible regio- and diastereoisomers, and the lowest energy conformer in each cluster is defined as the target transition state. The energies of the transition states are then compared to evaluate the most favorable reaction pathway (Step 5).

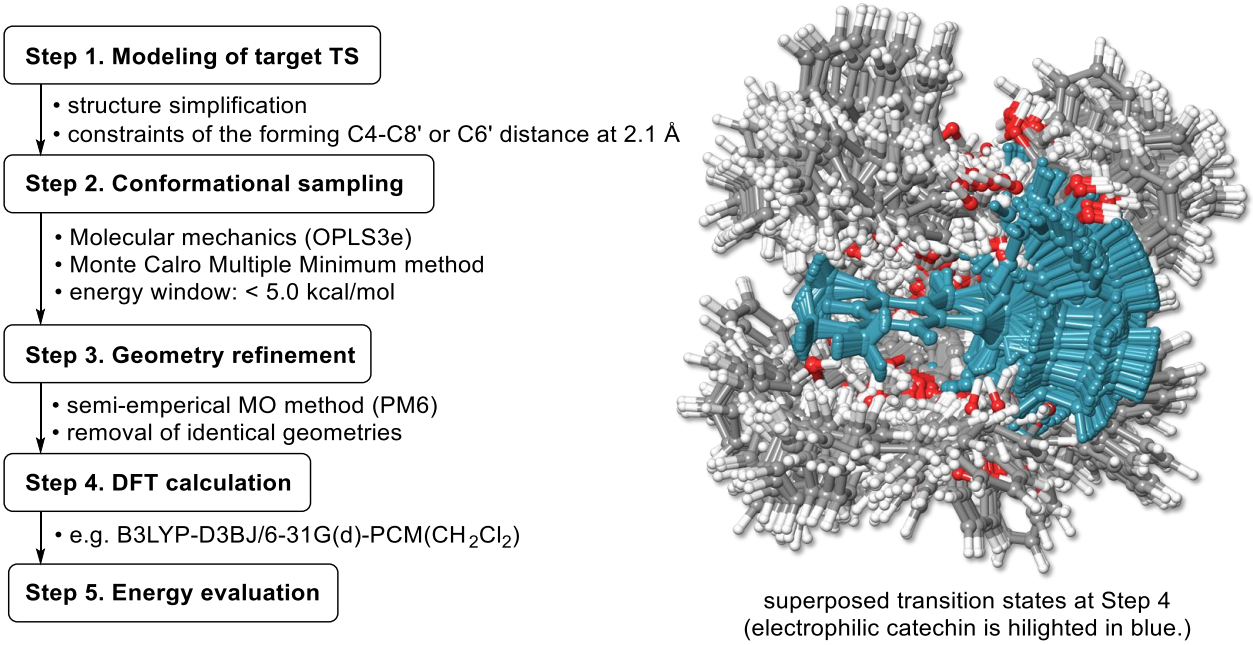

Scheme 2. Procedure for systematic search for transition states

3-3. Transition States for Intermolecular Interflavan Bond Formation in the Catechin Derivatives

In 2002, the Saito and Nakajima group reported the coupling of catechin derivatives **10** and **11**.[22] Compound **10** has an OEE leaving group at the C4 position, and the C3-hydroxy group and phenolic hydroxy groups are protected as acetate and benzyl ethers, respectively. The C3-hydroxy group of **11** is unprotected and the other hydroxy groups are protected as benzyl ethers. TMSOTf was used as a Lewis acid at −78 °C to mediate the intermolecular coupling of **10** and **11** to provide **12**. The coupling exclusively formed the C4-C8′ interflavan bond, and its regioisomer with the C4-C6′ bond was not observed under the reaction conditions. Furthermore, the C4-stereoselectively was controlled to construct the *trans*-C3,4 system with a trace amount of the corresponding *cis*-C3,4-diastereoisomer (dr = >48:1). The obtained **12** was used for the total synthesis of procyanidin B3.

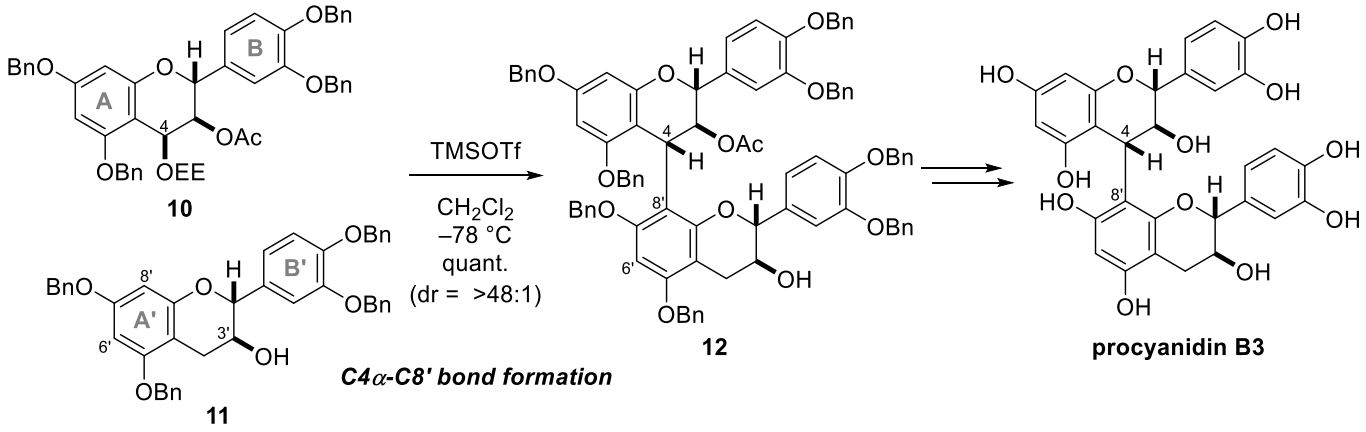

Scheme 3. C4α-C8′ Bond formation during synthesis of procyanidin B3 (Ref. 22)

The selective formation of the C4α-C8′ bond over C4β-C8′ and C4-C6′ bonds was examined by a computational evaluation of the transition states. For the calculation, the structures of both **10** and **11** were simplified by replacing the Ph groups of Bn on the A- and A′ rings and the OBn groups on the B- and B′-rings with H atoms. A systematic search of transition states with respect to C4-C8′ and C4-C6′ bond formation successfully identified **TS-G**, **TS-H** and **TS-I** from a total of 233 transition states as the lowest energy transition states that lead to the formation of C4α-C8′, C4β-C8′ and C4α-C6′ bonds, respectively (Figure 3). The energies of the transition states indicate that the formation of C4α-C8′ bonds via **TS-G** is the most energetically favored pathway from the cationic intermediates, while **TS-H** and **TS-I** that lead to the C4-diastereomer and the regioisomer of the product via **TS-G**, respectively, are destabilized by 2.5 and 3.5 kcal·mol^{-1} ($\Delta\Delta G$). This computational outcome reproduces the experimental results in Scheme 3, where only **12** bearing the C4α-C8′ bond is obtained.

The optimum geometry of **TS-G** has a unique conformation, where two catechin derivatives appear to interact with each other via non-covalent interactions, despite the possible disadvantage of a steric crush. It is well accepted that non-covalent interactions, including attractive and van der Waals interactions involving hydrogen bonding, CH-π and π-π interactions, play an important role in affecting the conformational preference.[26] Therefore, the origins of the stability of **TS-G** were investigated with a focus on the participation of non-covalent interactions. Although the complex geometry of **TS-G** complicates the investigation, the use of NCIPLOT,[27] a tool for visualizing non-covalent interactions that contribute to geometry stabilization, allowed the identification of a plausible origin of the low energy. As shown in Figure 4, the NCIPLOT map for **TS-G** has an extended green surface, which indicates the presence of non-covalent interactions that stabilize the structure. In particular, a clear CH-π interaction between H3 and the A′-ring, and a π-π interaction between the A- and B′-rings, are notable. Several

non-classical hydrogen bonds including C=O···H3 and C5-O···H8′ are also observed as green to blue surfaces that contribute to the stabilization of **TS-G**.

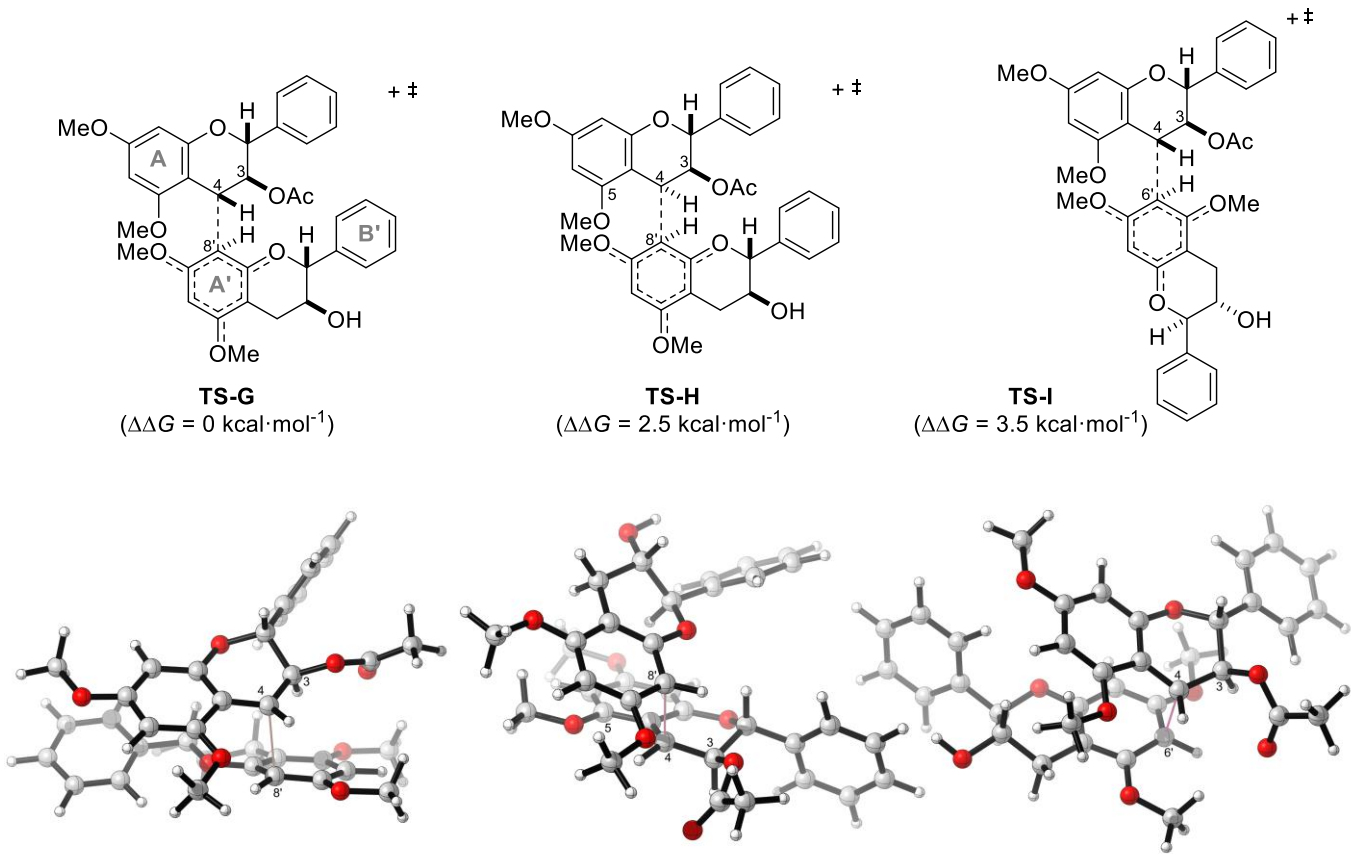

Figure 3. Lowest-energy transition states **TS-G**, **TS-H** and **TS-I** from 233 conformational isomers for C4α-C8′, C4β-C8′ and C4-C6′ bond formation, respectively

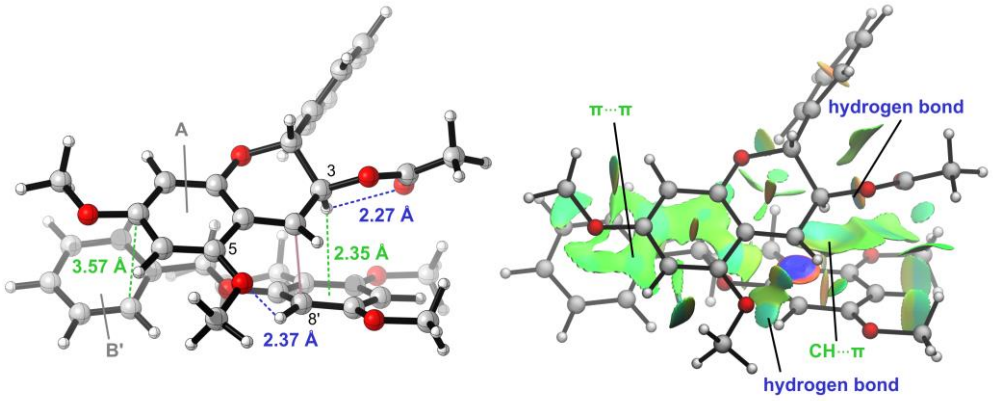

Figure 4. Non-covalent interactions visualized by NCIPLOT for **TS-G**. The forming bond, hydrogen bonds and π-π interactions are represented as pink, blue and green lines, respectively (left). Blue, green and red surfaces indicate attractive, van der Waals, and repulsive interactions, respectively (right).

3-4. Transition States for Intramolecular Interflavan Bond Formation in 5-Carbon-tethered Flavan-3-ols

The intermolecular approach for various combinations of flavan-3-ols affords the isomeric coupling products at the C3 and C3′ positions, which serve as advanced intermediates that lead to procyanidins B1-B4. On the other hand, the intermolecular reactions generate a considerable amount of trimeric and tetrameric side-products because the nucleophilic properties at the C8-position of the coupled products allow further reaction with the electrophile in situ. To overcome this drawback, an intramolecular approach using tethered flavan-3-ols **13** (catechin + catechin), **15** (catechin + epicatechin), and **17** (epicatechin + catechin) with a 5-carbon diacyl chain was developed (Scheme 4).[23] This strategy successfully led to the formation of the desired dimeric flavan-3-ol products without the undesired polymers. Of interest is that the C4-stereoselectivity in the intramolecular couplings is not exactly the same as that in the intermolecular couplings. A sharp contrast is the reaction of tethered flavan-3-ol **13** providing **14** with the *cis*-C3,4-disubstituent, a synthetic precursor for naturally occurring C4-epi procyanidin B3, and the coupling of non-tethered flavan-3-ols **10** and **11** affording **12** with the *trans*-C3,4-disubstituent (Schemes 3 and 4). The diacyl chain alters the C4-stereoselectivity of the coupling, and clearly affects the conformational preference of the transition states, whereas the reactions of **15** and **17** provided products **16** and **18** with the *trans*-C3,4-disubstituents, which have the same C4-stereoselectivity in the intermolecular couplings of the corresponding flavan-3-ols.

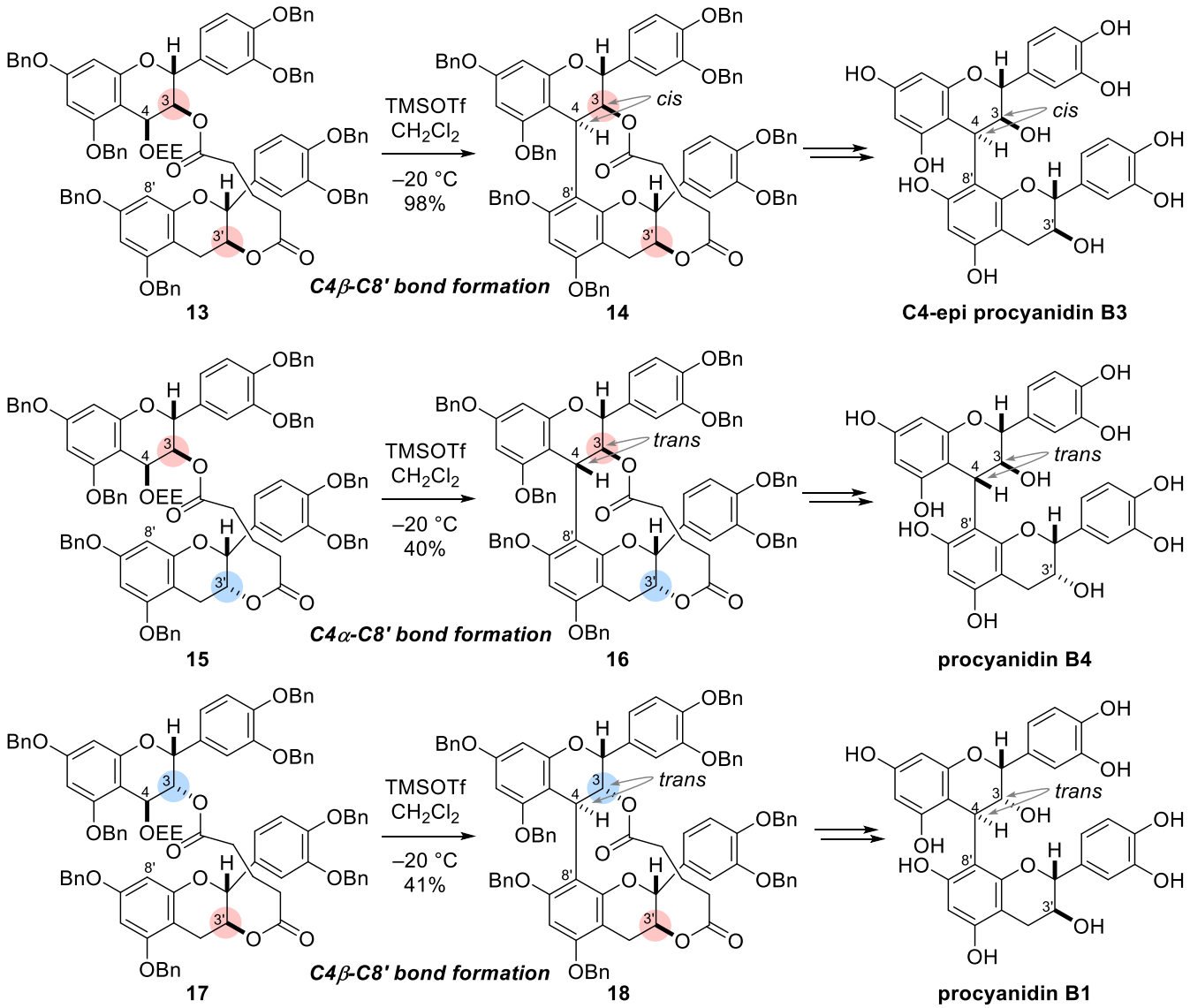

Scheme 4. Intramolecular C4-C8′ bond formation for 5-carbon-tethered flavan-3-ols **13**, **15** and **17** (Ref. 23)

The systematic search enabled identification of reasonable transition states to reproduce the C4-stereoselectivity for each reaction in Scheme 4. Among several DFT-optimized geometries obtained as models of the transition states for each C-C bond formation from carbocation intermediates, **TS-J**, **TS-K**, or **TS-L** was identified as having the lowest energy. Deprotonative rearomatization after C-C bond formation removes the C8′-stereocenters, so that the *cis*-C3,4-disubstituent is formed via **TS-J** and the *trans* system is formed via **TS-K**, or **TS-L**. The higher energy barriers for the other obtained isomeric transition states for each C-C bond indicates no formation of the C4-diastereomers.

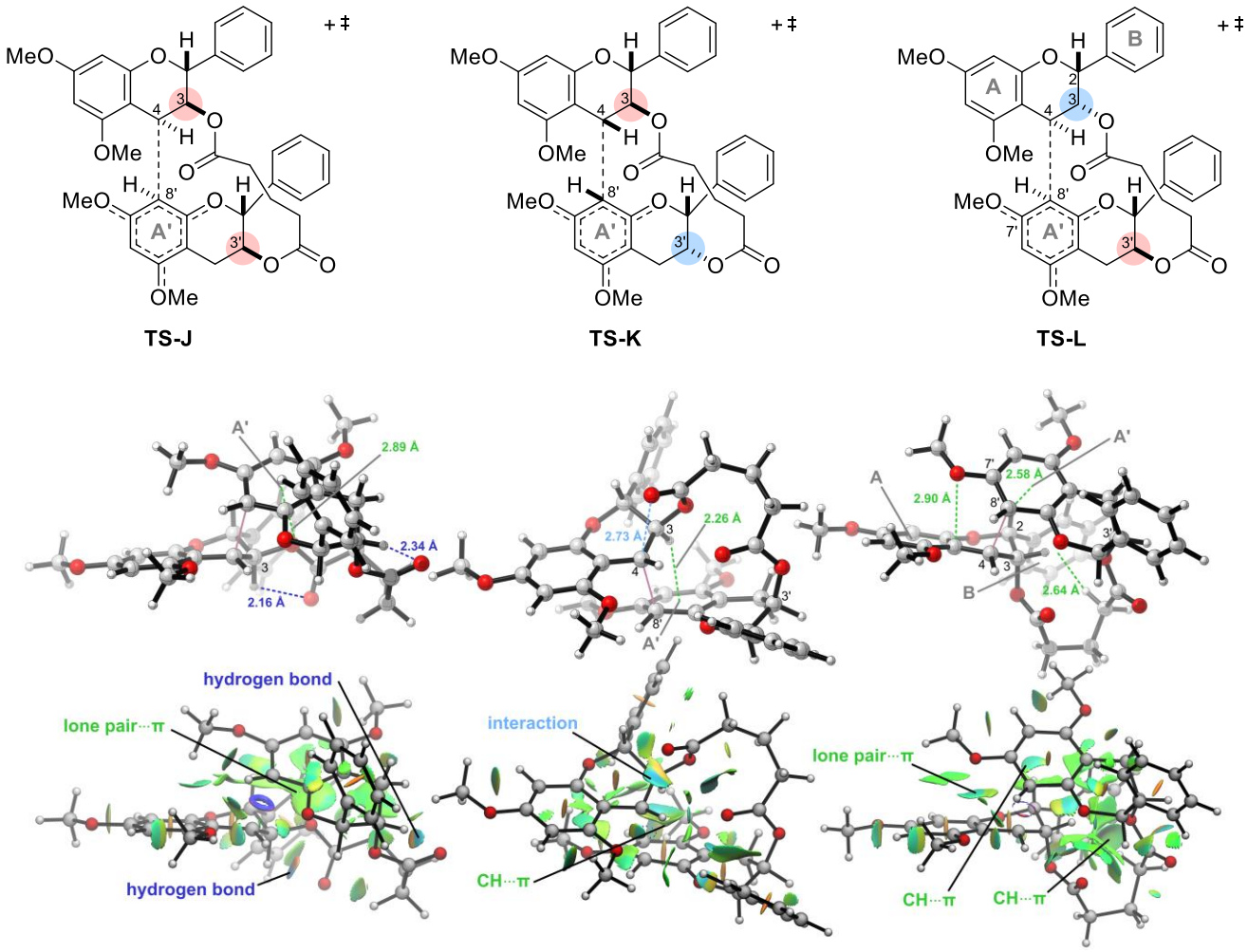

Figure 5. Lowest-energy transition states **TS-J**, **TS-K** and **TS-L** from 9, 6, and 7 conformational isomers for three intramolecular C4-C8′ bond formations, and their NICPLOTs. The forming bond, hydrogen bonds and van der Waals interactions are represented as pink, blue and green lines, respectively (middle). Blue, green and red surfaces indicate attractive, van der Waals, and repulsive interactions, respectively (bottom).

The NCIPLOT maps of the transition states **TS-J**, **TS-K** and **TS-L** show that the non-covalent interactions are attributable to the low energy of the geometries. In **TS-J**, a clear lone-pair π interaction between C3-O and the A′-ring is shown as a green surface. This interaction may allow the unique conformation of **TS-J**, where the nucleophile approaches from the same side as the C3-oxygen functional group. Several non-classical hydrogen bonds, particularly emphasized by H3···O=C and H3′···O=C, are included as blue surfaces, which also assist the conformational preference. In **TS-K**, a strong CH-π interaction occurs between H3 and the A′-ring, which would contribute to the preferential approach of the nucleophile from the opposite side of the C3-oxygen. In **TS-K**, a donor-acceptor-like interaction occurs between the C=O at C3 and cationic C4, which is represented as a blue surface. For **TS-L**, the

hydrogen in methylene adjacent to the carbonyl group and the B-ring undergo a strong CH-π interaction, and the other CH-π interactions between H2 and the A′-ring, and the lone-pair π interaction between C7′-O and the A-ring, as well as several hydrogen bonds, are indicated by the green surface.

The transition states for these intramolecular reactions of flavan-3-ols involve multiple van der Waals interactions, which are weak but non-negligible for stabilization of the conformations. Various different interactions occur depending on the 3D structure of the transition states; therefore, the role of weak interactions must be discussed individually for each transition state. The systematic search provides unique 3D structures for the transition states from many candidate conformational isomers, and allows discussion of the specific role of the weak interactions in each case.

3-5. Transition States for Intramolecular Interflavan Bond Formation in 9-Carbon-tethered Catechin Derivatives

The Saito and Nakajima group reported the effect of the diacyl chain, which enables switching of the regioselectivity of the intramolecular coupling of flavan-3-ols from C4-C8′ bond formation to C4-C6′ bond formation. Instead of the 5-carbon diacyl chain connecting the C3 and C3′-hydroxy groups during intramolecular C4-C8′ bond formation, a 9-carbon diacyl chain was employed to connect the C3 and C5′ hydroxy groups to the C4-C6′ interflavan bond (Scheme 5).[24] The $SnCl_4$-promoted coupling of **19** provided **20** in 72% yield as a single product without the formation of either its regio- or C4-diastereoisomers, and **20** was then used as an intermediate for the total synthesis of procyanidin B6. This is a notable example of selective C4-C6′ bond formation by the coupling of flavan-3-ols because there have been many reports that the coupling of flavan-3-ols preferably forms C4-C8′ bonds rather than C4-C6′ bonds.[28]

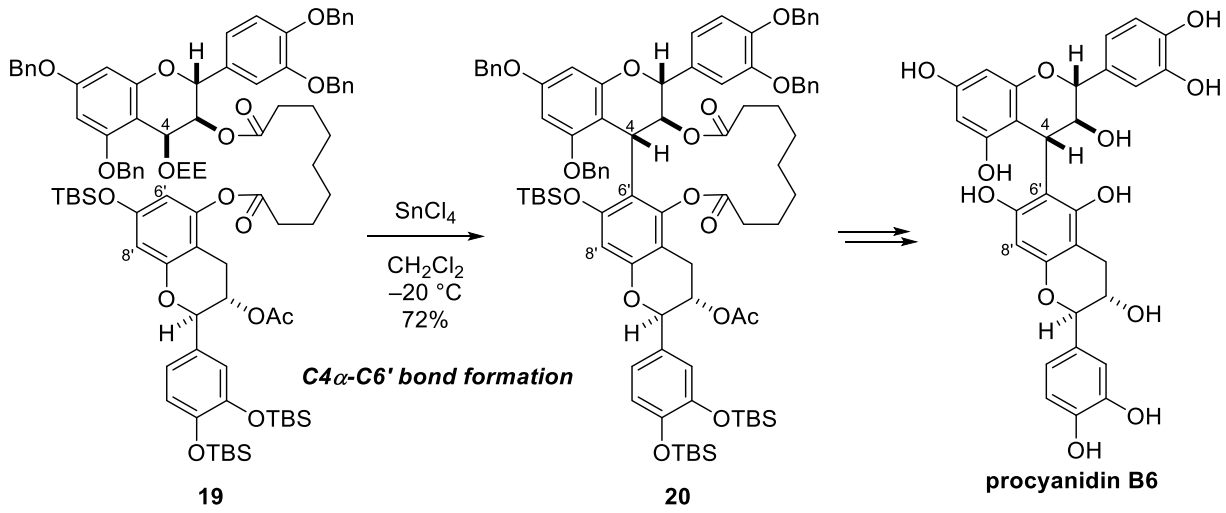

Scheme 5. Intramolecular C4-C6′ bond formation in 9-carbon tethered catechin derivative **19** (Ref. 24)

The search for transition states in intramolecular reactions is a challenge because the 9-carbon chain is involved in the formation of a large 15-membered ring, which provides a considerable amount of possible conformational isomers. This systematic search successfully identified **TS-M** as the lowest-energy transition state from 288 states, which led to C4α-C6′ bond formation (Figure 6). To explore the energy difference between C4-C6′ and C4-C8′ bond formation, a further search was performed for transition states that lead to the regioisomer with a C4-C8′ bond to identify **TS-N** from 79 transition states. The energy of **TS-N** is higher than that of **TS-M** ($\Delta\Delta G$ = 2.0 kcal/mol), which demonstrates that C4-C6′ bond formation is a more favorable pathway in the coupling of **19**, as seen from the experimental results in Scheme 5.

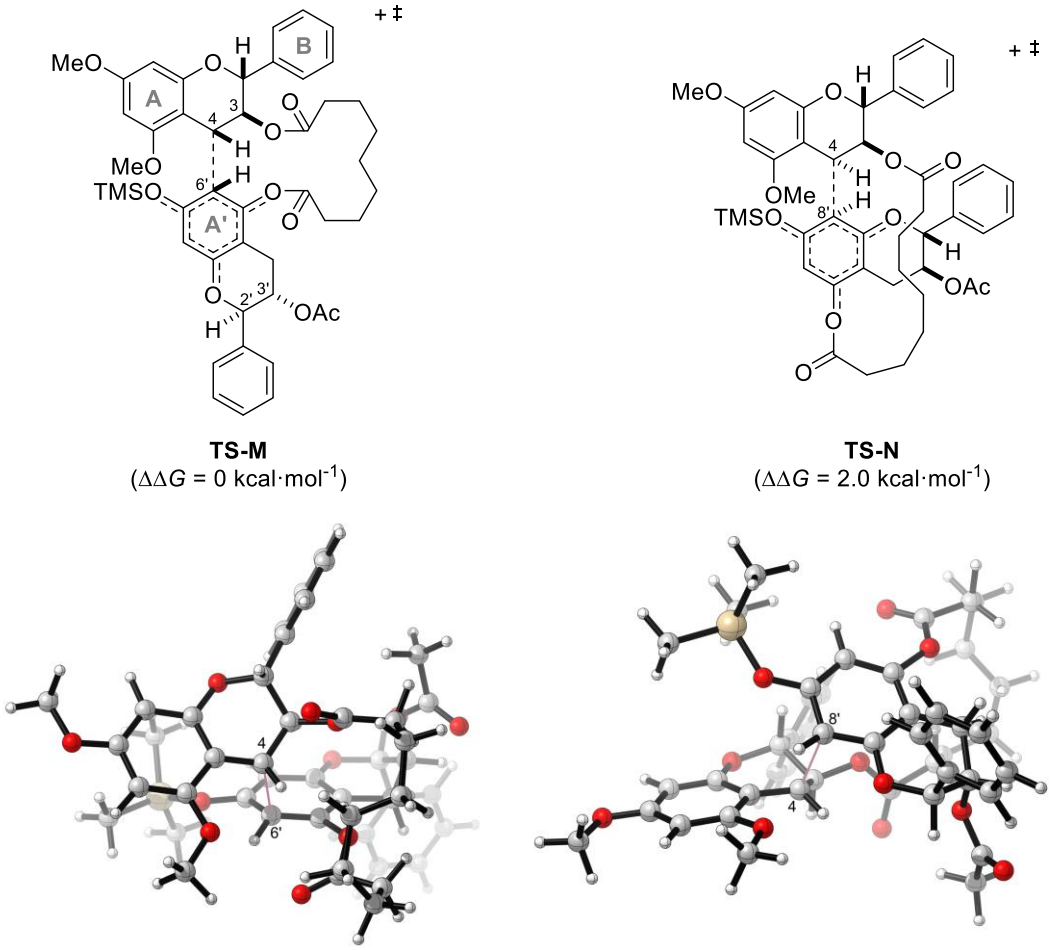

Figure 6. Lowest-energy transition states **TS-M** and **TS-N** from 288 and 79 conformational isomers for intramolecular C4-C6′ and C4-C8′ bond formation, respectively

The green surfaces in the NCIPLOT map for **TS-M** show multiple CH-π and lone-pair π interactions that contribute to the lowest energy of **TS-M** (Figure 7). The CH-π interactions between the Me of the axial C3′-acetate with the B-ring, and between H3 and the A′-ring, and the lone-pair π interaction between O7′

and the A-ring, are clearly evident. Although the two bulky C2′-phenyl and C3′-acetoxy groups are axial, the multiple weak interactions eventually stabilize the unique conformation of **TS-M**.

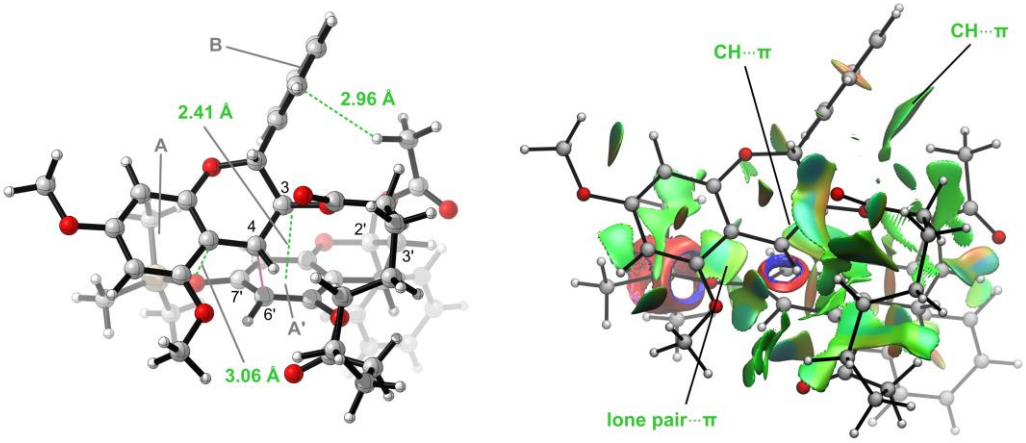

Figure 7. Non-covalent interactions of **TS-M** visualized by NCIPLOT. The forming bond and van der Waals interactions are represented as pink and green lines, respectively (left). Blue, green and red surfaces indicate attractive, van der Waals, and repulsive interactions, respectively (right).

4. CONCLUSION

In this review, our recent work on the systematic search for transition states and its application to analysis of regio- and stereoselective interflavan bond formation in flavan-3-ols is summarized. The method features a combination of conformational searches of constrained models to create a large library of transition state candidates and DTF-based transition state calculations. Using this procedure, reasonable transition states that reproduce the selectivities during inter- and intramolecular interflavan bond formation reported by the Saito and Nakajima group are obtained. The specific roles of van der Waals interactions in each transition state can be visualized by NCIPLOT mapping to demonstrate the importance of weak interactions for the conformational preference of transition states and selective interflavan bond formation.

Although DFT-based analysis of complex molecules such as those described in this review still requires a large amount of machine time at the current performance level of mainframe computers, we expect that technological advances driven by Moore's law will allow such computations to become routine, not only to gain insight into the reaction mechanisms of large molecules, but also to predict the reactivities of synthetic intermediates involved in the synthesis of natural products. This could enable accurate predictions of appropriate synthetic routes that match the requirements of synthetic chemists, such as shortest target-oriented synthesis, divergent oriented synthesis, and synthesis that utilize original transformations. Along with significant developments in database-driven planning of synthetic routes,[29,30]

we consider that further application of the present method based on systematic searches for transition states will be another effective approach toward planning the syntheses of natural products.

ACKNOWLEDGEMENTS

This research was financially supported by a Grant-in-Aid for Young Scientists (A) (No. 16H06213) from the Japan Society for the Promotion of Science (JSPS). We thank Professors Akiko Saito (Osaka Electro-Communication University) and Noriyuki Nakajima (Toyama Prefectural University) for many helpful suggestions and valuable discussion.

REFERENCES

1. For recent applications of transition state calculation in biosynthetic pathways of natural products, see: H. Sato, T. Mitsuhashi, M. Yamazaki, I. Abe, and M. Uchiyama, *Angew. Chem. Int. Ed.*, 2018, **57**, 14752; I. Fujii, M. Hashimoto, K. Konishi, A. Unezawa, H. Sakuraba, K. Suzuki, H. Tsushima, M. Iwasaki, S. Yoshida, A. Kudo, R. Fujita, A. Hichiwa, K. Saito, T. Asano, J. Ishikawa, D. Wakana, Y. Goda, A. Watanabe, M. Watanabe, Y. Masumoto, J. Kanazawa, H. Sato, and M. Uchiyama, *Angew. Chem. Int. Ed.*, 2020, **59**, 8464; L. Lauterbach, B. Goldfuss, and J. S. Dickschat, *Angew. Chem. Int. Ed.*, 2020, **59**, 11943; C. Zhang, X. Wang, Y. Chen, Z. He, P. Yu, and Y. Liang, *J. Org. Chem.*, 2020, **85**, 9440. For related studies from the Tantillo group, see reviews in ref. 2.
2. D. J. Tantillo, *Nat. Prod. Rep.*, 2011, **28**, 1035; D. J. Tantillo, *Comput. Mol. Sci.*, 2020, **10**, e1453.
3. For recent examples on analyses of the transition states of key transformations in natural product synthesis, see: D. T. Hog, F. M. E. Huber, G. Jiménez-Osés, P. Mayer, K. N. Houk, and D. Trauner, *Chem. Eur. J.*, 2015, **21**, 13646; J. H. Boyce, V. Eschenbrenner-Lux, and J. A. Porco, Jr., *J. Am. Chem. Soc.*, 2016, **138**, 14789; L. Xu, F. Liu, L.-W. Xu, Z. Gao, and Y.-M. Zhao, *Org. Lett.*, 2016, **18**, 3698; W. Liu, H. Li, P.-J. Cai, Z. Wang, Z.-X. Yu, and X. Lei, *Angew. Chem. Int. Ed.*, 2016, **55**, 3112; G. Kim, M. J. Kim, G. Chung, H.-Y. Lee, and S. Han, *Org. Lett.*, 2018, **20**, 6886; B. Maiga-Wandiam, A. Corbu, G. Massiot, F. Sautel, P. Yu, B. W.-Y. Lin, K. H. Houk, and J. Cossy, *J. Org. Chem.*, 2018, **83**, 5975; X.-S. Xue, B. J. Levandowski, C. Q. He, and K. N. Houk, *Org. Lett.*, 2018, **20**, 6108; T. Tsutsumi, S. Karanjit, A. Nakayama, and K. Namba, *Org. Lett.*, 2019, **21**, 2620; C. W. Lee, B. L. H. Taylor, G. P. Petrova, A. Patel, K. Morokuma, K. N. Houk, and B. M. Stoltz, *J. Am. Chem. Soc.*, 2019, **141**, 6995; M. Elkin, A. C. Scruse, A. Turlik, and T. R. Newhouse, *Angew. Chem. Int. Ed.*, 2019, **58**, 1025; H. Quintela-Varela, C. S. Jamieson, Q. Shao, K. N. Houk, and D. Trauner, *Angew. Chem. Int. Ed.*, 2020, **59**, 5263; M. Breunig, P. Yuan, and T. Gaich, *Angew. Chem. Int. Ed.*, 2020, **59**, 5521; K. M. Lambert, J. B. Cox, L. Liu, A. C. Jackson, S. Yruegas, K. B. Wiberg, and J. L. Wood, *Angew. Chem. Int. Ed.*, 2020, **59**, 9757.

4. For early examples on computational design of intermediates toward natural product syntheses, see: T. Takahashi, K. Shimizu, T. Doi, J. Tsuji, and Y. Fukazawa, *J. Am. Chem. Soc.*, 1988, **110**, 2674; T. Doi, Y. Miura, S. Kawauchi, and T. Takahashi, *Chem. Commun.*, 2005, 4908. For recent examples, see: D. J. Tao, Y. Slutskyy, M. Muuronen, A. Le, P. Kohler, and L. E. Overman, *J. Am. Chem. Soc.*, 2018, **140**, 3091; D. E. Kim., J. E. Zweig, and T. R. Newhouse, *J. Am. Chem. Soc.*, 2019, **141**, 1479.
5. M. Elkin and T. R. Newhouse, *Chem. Soc. Rev.*, 2018, **47**, 7830.
6. L. W. Chung, W. M. C. Sameera, R. Ramozzi, A. J. Page, M. Hatanaka, G. P. Petrova, T. V. Harris, X. Li, Z. Ke, F. Liu, H.-B. Li, L. Ding, and K. Morokuma, *Chem. Rev.*, 2015, **115**, 5678; Q. Peng and R. S. Paton, *Acc. Chem. Res.*, 2016, **49**, 1042; S. Ahn, M. Hong, M. Sundararajan, D. H. Ess, and M.-H. Baik, *Chem. Rev.*, 2019, **119**, 6509.
7. T. Sperger, I. A. Sanhueza, I. Kalvet, and F. Schoenebeck, *Chem. Rev.*, 2015, **115**, 9532; S.-C. Qi, J. Hayashi, and L. Zhang, *RSC Adv.*, 2016, **6**, 77375; S. Santoro, M. Kalek, G. Huang, and F. Himo, *Acc. Chem. Res.*, 2016, **49**, 1006; Y. Park, S. Ahn, D. Kang, and M.-H. Baik, *Acc. Chem. Res.*, 2016, **49**, 1263; X. Zhang, L. W. Chung, and Y.-D. Wu, *Acc. Chem. Res.*, 2016, **49**, 1302; T. Sperger, I. A. Sanhueza, and F. Schoenebeck, *Acc. Chem. Res.*, 2016, **49**, 1311; Y.-F. Yang, X. Hong, J.-Q. Yu, and K. N. Houk, *Acc. Chem. Res.*, 2017, **50**, 2853; D. L. Davies, S. A. Macgregor, and C. L. McMullin, *Chem. Rev.*, 2017, **117**, 8649; I. Funes-Ardoiz and F. Maseras, *ACS Catal.*, 2018, **8**, 1161; Y. Takeda, W. M. C. Sameera, and S. Minakata, *Acc. Chem. Res.*, 2020, **53**, 1686.
8. P. H.-Y. Cheong, C. Y. Legault, J. M. Um, N. Çelebi-Ölçüm, and K. N. Houk, *Chem. Rev.*, 2011, **111**, 5042; Y.-h. Lam, M. N. Grayson, M. C. Holland, A. Simon, and K. N. Houk, *Acc. Chem. Res.*, 2016, **49**, 750; K. S. Halskov, B. S. Donslund, B. M. Paz, and K. A. Jørgensen, *Acc. Chem. Res.*, 2016, **49**, 974; R. B. Sunoj, *Acc. Chem. Res.*, 2016, **49**, 1019; G. Tanriver, B. Dedeoglu, S. Catak, and V. Aviyente, *Acc. Chem. Res.*, 2016, **49**, 1250; D. M. Walden, O. M. Ogba, R. C. Johnston, and P. H.-Y. Cheong, *Acc. Chem. Res.*, 2016, **49**, 1279.
9. C. S. Jamieson, M. Ohashi, F. Liu, Y. Tang, and K. N. Houk, *Nat. Prod. Rep.*, 2019, **36**, 698.
10. E. Hansen, A. R. Rosales, B. Tutkowski, P.-O. Norrby, and O. Wiest, *Acc. Chem. Res.*, 2016, **49**, 996; S. E. Wheeler, T. J. Seguin, Y. Guan, and A. C. Doney, *Acc. Chem. Res.*, 2016, **49**, 1061; A. F. Zahrt, S. V. Athavale, and S. E. Denmark, *Chem. Rev.*, 2019, **120**, 1620.
11. S. Hashimoto, S. Katoh, T. Kato, D. Urabe, and M. Inoue, *J. Am. Chem. Soc.*, 2017, **139**, 16420; K. Hagiwara, T. Tabuchi, D. Urabe, and M. Inoue, *Chem. Sci.*, 2016, **7**, 4372; T. Asaba, Y. Katoh, D. Urabe, and M. Inoue, *Angew. Chem. Int. Ed.*, 2015, **54**, 14457.
12. K. Fukaya, A. Saito, N. Nakajima, and D. Urabe, *J. Org. Chem.*, 2019, **84**, 2840; K. Fukaya, A. Saito, N. Nakajima, and D. Urabe, *J. Org. Chem.*, 2020, **85**, 5010; K. Fukaya, A. Saito, N. Nakajima, and D. Urabe, *Bull. Chem. Soc. Jpn.*, 2020, **93**, 1107.

13. S. Maeda, K. Ohno, and K. Morokuma, *Phys. Chem. Chem. Phys.*, 2013, **15**, 3683; W. M. C. Sameera, S. Maeda, and K. Morokuma, *Acc. Chem. Res.*, 2016, **49**, 763.
14. G. Henkelman and H. Jónsson, *J. Chem. Phys.*, 2000, **113**, 9978.
15. P. Vidossich, A. Lledós, and G. Ujaque, *Acc. Chem. Res.*, 2016, **49**, 1271.
16. Experimentally, the formation of a 64:36 mixture of **2a** and its *trans* isomer from **1a** in 68 h at 140 °C is reported. See, D. A. Smith, K. Sakan, and K. N. Houk, *Tetrahedron Lett.*, 1986, **27**, 4877.
17. J. B. Harborne and H. Baxter, The Handbook of Natural Flavonoids Vol. 2, John Wiley & Sons, Inc.: New York, NY, USA, 1999.
18. J. Jankun, S. H. Selman, R. Swiercz, and E. Skrzypczak-Jankun, *Nature*, 1997, **387**, 561; P. Cos, T. De Bruyne, N. Hermans, S. Apers, D. Vanden Berghe, and A. J. Vlietinck, *Curr. Med. Chem.*, 2004, **11**, 1345; C. Selmi, T. K. Mao, C. L. Keen, H. H. Schmitz, and M. E. Gershwin, *J. Cardiovasc. Pharmacol.*, 2006, **47**, S163; V. Nandakumar, T. Singh, and S. K. Katiyar, *Cancer Lett.*, 2008, **269**, 378; N. Gonzalez-Abuin, M. Pinent, A. Casanova-Marti, L. Arola, M. Blay, and A. Ardevol, *Curr. Med. Chem.*, 2015, **22**, 39.
19. P. V. Gadkari and M. Balaraman, *Food Bioprod. Process.*, 2015, **93**, 122.
20. A. Saito, Y. Doi, A. Tanaka, N. Matsuura, M. Ubukata, and N. Nakajima, *Bioorg. Med. Chem.*, 2004, **12**, 4783; A. Saito and N. Nakajima, *Heterocycles*, 2010, **80**, 1081.
21. For total synthesis of procyanidin B series, see: W. Tückmantel, A. P. Kozikowski, and L. J. Romanczyk, *J. Am. Chem. Soc.*, 1999, **121**, 12073; I. Tarascou, K. Barathieu, Y. André, I. Pianet, E. J. Dufourc, and E. Fouquet, *Eur. J. Org. Chem.*, 2006, 5367; P. K. Sharma, A. Kolchinski, H. A. Shea, J. J. Nair, Y. Gou, L. J. Romanczyk, and H. H. Schmitz, *Org. Process Res. Dev.*, 2007, **11**, 422; K. Oyama, M. Kuwano, M. Ito, K. Yoshida, and T. Kondo, *Tetrahedron Lett.*, 2008, **49**, 3176; M. C. Achilonu, S. L. Bonnet, and J. H. van der Westhuizen, *Org. Lett.*, 2008, **10**, 3865; Y. Mohri, M. Sagehashi, T. Yamada, Y. Hattori, K. Morimura, Y. Hamauzu, T. Kamo, M. Hirota, and H. Makabe, *Heterocycles*, 2009, **79**, 549; G. Watanabe, K. Ohmori, and K. Suzuki, *Chem. Commun.*, 2013, **49**, 5210.
22. A. Saito, N. Nakajima, A. Tanaka, and M. Ubukata, *Tetrahedron*, 2002, **58**, 7829; A. Saito, N. Nakajima, N. Matsuura, A. Tanaka, and M. Ubukata, *Heterocycles*, 2004, **62**, 479.
23. A. Saito, N. Nakajima, A. Tanaka, and M. Ubukata, *Tetrahedron Lett.*, 2003, **44**, 5449; A. Saito, N. Nakajima, A. Tanaka, and M. Ubukata, *Heterocycles*, 2003, **61**, 287; A. Saito, A. Tanaka, M. Ubukata, and N. Nakajima, *Synlett*, 2004, 2040.
24. Y. Higashino, T. Okamoto, K. Mori, T. Kawasaki, M. Hamada, N. Nakajima, and A. Saito, *Molecules*, 2018, **23**, 205.
25. M. G. Medvedev, M. V. Panova, G. G. Chilov, I. S. Bushmarinov, F. N. Novikov, O. V. Stroganov, A.

A. Zeifman, and I. V. Svitanko, *Mendeleev Commun.*, 2017, **27**, 224; M. G. Medvedev, A. A. Zeifman, F. N. Novikov, I. S. Bushmarinov, O. V. Stroganov, I. Y. Titov, G. G. Chilov, and I. V. Svitanko, *J. Am. Chem. Soc.*, 2017, **139**, 3942; Y. Guan, V. M. Ingman, B. J. Rooks, and S. E. Wheeler, *J. Chem. Theory Comput.*, 2018, **14**, 5249.

26. M. Egli and S. Sarkhel, *Acc. Chem. Res.*, 2007, **40**, 197; O. Takahashi, Y. Kohno, and M. Nishio, *Chem. Rev.*, 2010, **110**, 6049; A. J. Neel, M. J. Hilton, M. S. Sigman, and F. D. Toste, *Nature*, 2017, **543**, 637.
27. E. R. Johnson, S. Keinan, P. Mori-Sánchez, J. Contreras-García, A. J. Cohen, and W. Yang, *J. Am. Chem. Soc.*, 2010, **132**, 6498; J. Contreras-García, E. R. Johnson, S. Keinan, R. Chaudret, J.-P. Piquemal, D. N. Beratan, and W. Yang, *J. Chem. Theory Comput.*, 2011, **7**, 625.
28. G. Watanabe, K. Ohmori, and K. Suzuki, *Chem. Commun.*, 2014, **50**, 14371.
29. B. Liu, B. Ramsundar, P. Kawthekar, J. Shi, J. Gomes, Q. L. Nguyen, S. Ho, J. Sloane, P. Wender, and V. Pande, *ACS Cent. Sci.*, 2017, **3**, 1103; M. H. S. Segler, M. Preuss, and M. P. Waller, *Nature*, 2018, **555**, 604; T. Klucznik, B. Mikulak-Klucznik, M. P. McCormack, H. Lima, S. Szymkuć, M. Bhowmick, K. Molga, Y. Zhou, L. Rickershauser, E. P. Gajewska, A. Toutchkine, P. Dittwald, M. P. Startek, G. J. Kirkovits, R. Roszak, A. Adamski, B. Sieredzińska, M. Mrksich, S. L. J. Trice, and B. A. Grzybowski, *Chem.*, 2018, **4**, 522.
30. S. Szymkuć, E. P. Gajewska, T. Klucznik, K. Molga, P. Dittwald, M. Startek, M. Bajczyk, and B. A. Grzybowski, *Angew. Chem. Int. Ed.*, 2016, **55**, 5904; C. W. Coley, W. H. Green, and K. F. Jensen, *Acc. Chem. Res.*, 2018, **51**, 1281.

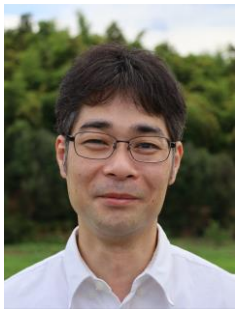

Daisuke Urabe received his Ph.D. degree in 2006 from Nagoya University under the supervision of Professors Minoru Isobe and Toshio Nishikawa. He then carried out postdoctoral research with Professor Yoshito Kishi at Harvard University (2006-2007). In 2008, he moved to the University of Tokyo as an assistant professor in the research group of Professor Masayuki Inoue, and was promoted to a lecturer in 2013. In 2017, he moved to Toyama Prefectural University as a professor to start an independent carrier. He was awarded the Young Scientist's Research Award in Natural Product Chemistry in 2013, Thieme Chemistry Journal Award 2014, and The Pharmaceutical Society of Japan Award for Young Scientists in 2015. His research interests include the total synthesis of natural products, and theoretical chemistry of complex reaction systems.

Keisuke Fukaya obtained a B.S. degree from Keio University (2012), where he conducted undergraduate research with Professor Noritaka Chida. He received a Ph.D. degree from the same university for work in the area of natural product synthesis under the joint supervision of Professor Noritaka Chida and Professor Takaaki Sato (2017). He then carried out postdoctoral research at the University of Texas at Austin under the supervision of Professor Michael J. Krische. In 2018, he joined the faculty at Toyama Prefectural University as an Assistant Professor. His research is focused on natural product synthesis and the development of computational approaches for the efficient synthesis of complex molecules.